

Graph Cuts for the Multiphase Mumford-Shah Model Using Piecewise Constant Level Set Methods *

Egil Bae[†] Xue-Cheng Tai[‡]

June 3, 2008

Abstract

Variational segmentation methods have been intensively studied. Traditionally, the Euler-Lagrange equations are solved by some iterative numerical methods. Normally, the speed is slow. In this work, the piecewise constant level set method (PCLSM) is used for the multiphase Mumford-Shah segmentation model. Instead of solving the Euler-Lagrange equations, we propose to solve the resulting minimization problem by graph cuts, a combinatorial optimization technique. By finding the minimum cut on a special graph, we obtain the solution for the segmentation problem. Numerical experiments show that the new approach is very superior in terms of efficiency, while maintaining the same quality of results.

1 Introduction

The level set method [18, 40] is a powerful tool for representing moving or stationary interfaces. The interface may typically be the solution of a geometric PDE or a geometric variational problem. The level set method has seen a remarkable number of applications in image analysis, fluid dynamics, inverse problems and computer vision [9, 8, 19, 39, 42]. The idea is to implicitly represent the interface as the zero level set of a function defined in a higher dimensional euclidian space. The geometric PDE or variational problem can then be redefined on functions in a euclidian space.

There are many options for constructing the level set function. Originally the signed distance function to the interface was used. As an alternative, the

*Support from the Norwegian Research Council (eVita project 166075), National Science Foundation of Singapore (NRF2007IDM-IDM002-010) and Ministry of Education of Singapore (Moe Tier 2 T207B2202) are gratefully acknowledged.

[†]Department of Mathematics, University of Bergen, Norway (Egil.Bae@math.uib.no).

[‡]Department of Mathematics, University of Bergen, Norway and Division of Mathematical Sciences, School of Physical and Mathematical Sciences, Nanyang Technological University, Singapore. (tai@mi.uib.no).

work of [34, 33, 45] proposed to use piecewise constant level set functions, representing the interfaces by discontinuities. This has certain advantages, such as eliminating the need for reinitialization of the level set function during evolution. Another important advantage is the ability to represent several interfaces by one single level set function. This method will be referred to as the piecewise constant level set method (PCLSM).

The papers [34, 33, 32, 45] deal with PCLSM for the Mumford-Shah model, which is an established variational model for image segmentation [38]. Mumford Shah image segmentation was also one of the first application areas of the level set method in computer vision. Chan and Vese [8] proposed to use the traditional level set method as a numerical realization for this model.

In this work we will review the relationship between the Mumford-Shah model [38], the Chan-Vese model [8] and the PCLSM [34]. Afterwards, we reveal a relationship between the piecewise constant level set method [34] and an integer optimization technique called graph cuts [29]. Graph cuts is a well-known technique in image analysis and computer vision [20, 5, 21, 2, 27, 28]. What makes graph cuts so powerful, is its efficiency and ability to find global minima. In the recent years, the relationship between graph cuts and variational problems has started to establish [3, 4, 17]. In this work we aim to further unify graph cuts and the level set method, and shrink the gap between some integer and continuous optimization problems. We will show that the multiphase Mumford-Shah functional can be minimized via graph cuts in the framework of PCLSM. To the best of our knowledge, we are the first to attempt this.

The paper is organized as follows. Section 2.3 starts by a review of the PCLSM and its application to Mumford-Shah image segmentation. In Section 3 we propose graph cuts as a new optimization method for the resulting minimization problems. Finally, in Section 4, experiments are set up, comparing the two approaches.

2 Previous work on PDE based image segmentation

In [7], a good survey has been given to PDE based image segmentation. Due to its wide range of applications for real problems, Mumford-Shah type of segmentation methods have been intensively studied in the past years. In the following, we review the Mumford-Shah model and the Chan-Vese model and then show the relationship with the PCLSM. Until now, it has been common to use some explicit time marching scheme to solve the equations resulting from these models. The convergence is normally slow. In the next section, we show that graph-cut type of integer minimization techniques can be used to get some faster algorithms.

2.1 Mumford-Shah model

The Mumford-Shah functional [38] is an established model for image segmentation problems. Let u^0 be a given image defined in the domain Ω . One seeks n interfaces Γ_i and an approximation image u that minimizes

$$E(u, \Gamma_i) = \int_{\Omega} (u - u^0)^2 dx + \mu \int_{\Omega \setminus \cup_i \Gamma_i} |\nabla u|^2 dx + \sum_{i=1}^n \nu \int_{\Gamma_i} ds. \quad (1)$$

For many applications, it is enough to assume that u is a piecewise constant function. For such cases, the second term disappears from the above minimization functional. Among the ways of representing the unknown interfaces, the level set method is the most elegant due to its ability to deal with unknown topology. Its main drawback is expensive computation.

2.2 Chan-Vese model

In [8], Chan and Vese proposed a level set method for numerical realization of the optimization problem (1), assuming that u is a piecewise constant function. In this approach, the unknown interfaces are represented by the zero level set of a Lipschitz continuous function $\phi(x) : \Omega \mapsto \mathbb{R}$. The idea is to express the functional (1) in terms of the level set function ϕ . One ends up with

$$\min_{\phi, c_1, c_2} \int_{\Omega} (|\nabla H(\phi)| + \lambda \{H(\phi)(c_1 - u^0)^2 + (1 - H(\phi))(c_2 - u^0)^2\}) dx, \quad (2)$$

where $H(\cdot) : \mathbb{R} \mapsto \mathbb{R}$ is the Heaviside function $H(x) = 0$ if $x < 0$ and $H(x) = 1$ if $x \geq 0$. The resulting Euler-Lagrange equation for ϕ is:

$$\phi_t = \delta(\phi) \left\{ \nabla \cdot \left(\frac{\nabla \phi}{|\nabla \phi|} \right) - \lambda \{ (c_1 - u^0)^2 - (c_2 - u^0)^2 \} \right\}, \quad (3)$$

The constant values c_1 and c_2 are updated in each iteration according to

$$c_1 = \frac{\int_{\Omega} H(\phi) u^0 dx}{\int_{\Omega} H(\phi) dx} \quad c_2 = \frac{\int_{\Omega} (1 - H(\phi)) u^0 dx}{\int_{\Omega} 1 - H(\phi) dx}. \quad (4)$$

For numerical simulations, the functions $H(\phi)$ and $\delta(\phi)$ are replaced by some smoothed regularizations. Often $\delta(\phi)$ is replaced with $|\nabla \phi|$. The gradient descent equation is solved using an explicit finite difference scheme. The above formulation differs a little from the original model [8], because we denote the constant values by \mathbf{c} .

The level set based algorithm of Chan and Vese can be extended to multi-phase piecewise constant models as in [49]. The idea is simply to introduce new level set functions to describe a greater number of regions using intersections between interiors and exteriors of the level sets [44]. One can then use the Heaviside function to express characteristic functions of the various regions that appear in the integrals of (2) in terms of these level set functions. Subsequently,

finding the Euler-Lagrange equations for the energy functional thus expressed in terms of level set functions yields a coupled system of non-linear parabolic PDEs to be solved by gradient descent. The details can be found in [49]. It must also be mentioned that some work has been made incorporating a priori shape information into the above functionals. The details can be found in [12, 13].

2.3 Piecewise constant level set method

One can also minimize the Mumford-Shah functional by PCLSM as in [34]. The PCLSM can be described as follows. One seeks a partitioning of the domain Ω into n subdomains $\{\Omega_i\}_{i=1}^n$ satisfying

$$\bigcap_{i=1}^n \Omega_i = \emptyset, \quad \bigcup_{i=1}^n \Omega_i = \Omega. \quad (5)$$

The subdomains Ω_i can be multiple connected. A partitioning of Ω as in (5) can be described in terms of a piecewise constant level set function ϕ

$$\phi = i \quad \text{in } \Omega_i \quad \text{for } i = 1, 2, \dots, n. \quad (6)$$

In contrast to the traditional level set method [40, 8], interfaces between the subdomains are represented as discontinuities in the level set function ϕ . Moreover, no more than one function ϕ is needed to represent any numbers of phases. It must be emphasized that the maximum number of phases n needs to be given in advance. Given a ϕ satisfying (6), it is possible to construct the characteristic functions ψ_i of each subdomain Ω_i by

$$\psi_i = \frac{1}{\alpha_i} \prod_{j=1, j \neq i} (\phi - j) \quad \text{with} \quad \alpha_i = \prod_{k=1, k \neq i} (i - k). \quad (7)$$

We can retrieve all the geometrical information of the boundaries of Ω_i from their characteristic functions. For example, these functions can be used to calculate the perimeter of the interfaces surrounding each subdomain Ω_i :

$$\text{Per}(\Gamma_i) = \int_{\Omega} |\nabla \psi_i| dx. \quad (8)$$

In addition, any piecewise constant function u can be written as a linear combination of the characteristic functions $\{\psi_i\}$

$$u = \sum_{i=1}^n c_i \psi_i. \quad (9)$$

Since ψ_i is extracted from ϕ , we see that u is completely characterized by the n scalars $\mathbf{c} = \{c_i\}_{i=1}^n$ and the level set function ϕ . It is easy to see that a function given in the form (9), is a piecewise constant function having values $u = c_i$ in Ω_i .

Following the ideas outlined above, the multiphase Mumford-Shah functional (1) can now be written in terms of the piecewise constant level set function ϕ

$$E(\mathbf{c}, \phi) = \sum_{i=1}^n \int_{\Omega} (u - u^0)^2 dx + \frac{\nu}{2} \sum_{i=1}^n \int_{\Omega} |\nabla \psi_i| dx. \quad (10)$$

The last term, which is the total variation of the characteristic function of each subdomain, measures the perimeters.

However, this approach of regularizing each characteristic function can slow down the convergence of the iterative scheme used for solving the minimization problem. Almost the same results can be obtained by regularizing the level set function ϕ directly (see for instance [45])

$$E(\mathbf{c}, \phi) = \sum_{i=1}^n \int_{\Omega} (u - u^0)^2 dx + \nu \int_{\Omega} |\nabla \phi| dx. \quad (11)$$

This approximation of the perimeters, is somewhat similar to the original multiphase approach of Chan and Vese [49]. There are some variants of the total variation regularization term. The commonly used version is the isotropic total variation

$$TV_2(\phi) = \int_{\Omega} |\nabla \phi|_2 dx = \int_{\Omega} \sqrt{|\phi_{x_1}|^2 + |\phi_{x_2}|^2} dx \quad (12)$$

In order to simplify computation, often a simpler version is used

$$TV_1(\phi) = \int_{\Omega} |\nabla \phi|_1 dx = \int_{\Omega} |\phi_{x_1}| + |\phi_{x_2}| dx. \quad (13)$$

However, since TV_1 is not isotropic, regularization will be stronger in certain directions. A more isotropic version based on the 1-norm can be obtained by splitting TV_1 between the original function, and one rotated counterclockwise $\pi/4$ radians, c.f [6, 41].

$$TV_{1, \frac{\pi}{4}}(\phi) = \frac{1}{2} \int_{\Omega} \{ |\nabla \phi(x)|_1 + |R_{\frac{\pi}{4}} \nabla \phi(x)|_1 \} dx. \quad (14)$$

Above, $R_{\frac{\pi}{4}}$ is the rotation matrix that rotates a vector $\pi/4$ radians in the counterclockwise direction. It is also possible to create even more isotropic versions by considering more such rotations. Previously, (10) or (11) have been minimized by continuous optimization techniques [34]. A function ϕ satisfies (6) if and only if it is a zero of the polynomial

$$K(\phi) = \prod_{i=1}^n (\phi - i). \quad (15)$$

i.e. $K(\phi) = 0$. Thus, in order to use ϕ to minimize the Mumford-Shah functional, we need to solve the following constrained optimization problem

$$\min_{\mathbf{c}, \phi} E(\mathbf{c}, \phi) \quad \text{subject to} \quad K(\phi) = 0.$$

This can be achieved by searching for a saddle point of the augmented lagrangian functional, c.f. [34]

$$L(\mathbf{c}, \phi, \lambda) = E(\mathbf{c}, \phi) + \int_{\Omega} \lambda K(\phi) dx + \frac{r}{2} \int_{\Omega} |K(\phi)|^2 dx, \quad (16)$$

where λ is a function defined on Ω and $r \in \mathbb{R}^+$. At the saddle point, the following Euler-Lagrange equations must be satisfied

$$\frac{\partial L}{\partial \phi} = 0, \quad \frac{\partial L}{\partial \lambda} = 0, \quad \frac{\partial L}{\partial c_i} = 0. \quad (17)$$

A common approach is to solve the above equations by a gradient decent time marching scheme with finite difference approximations. In [34], a gradient decent method was used to solve the equation (17). Several faster methods have been tested in [10, 31, 47, 45, 35, 11]. In [47, 46], Newton's method was used to accelerate the convergence. On the other hand, AOS method [36, 37, 50] was used in [31, 11] to get faster algorithms for equations (17). We shall also mention that multigrid methods [10] and MBO type of projection methods [45] can be used to solve the equations (17). In this work, we use graph cuts to solve the minimization problem. Numerical experiments show that this algorithm is many times faster than the afore mentioned acceleration schemes. Some fast curve evolution methods that do not involve PDEs have also recently been proposed [43], although these seem to have a bit of trouble for very noisy images.

2.4 Relations between the methods

We can see that the Chan-Vese model [8, 49] is essentially trying to use the level set method [40] for the Mumford shah segmentation model, while the work [34] is trying to use PCLSM for the Mumford-Shah model. Both the CVM and the PCLSM are trying to use different mathematical methods to solve the same problem. They produce different nonlinear partial differential equations in the continuous setting. Comparisons between PCLSM and CVM have been done in [34, 33, 11, 47]. Compared with CVM, the minimization functional of PCLSM is convex and it avoids the use the Heaviside function and also the re-initialization procedure of the traditional level set method. PCLSM can also identify an arbitrary number of phases with just one function.

3 Integer optimization for PCLSM

Minimizing (10) or (11) by continuous optimization methods require us to add the constraint $K(\phi) = 0$ to force ϕ to take only integer values. We instead propose the much more natural approach of using integer optimization to solve (11). Instead of discretizing the Euler-Lagrange equations, we will discretize the variational problem (11). This results in an energy function, which we show can be minimized by a graph-cut algorithm in case the values \mathbf{c} are known. Finally, an algorithm is designed to minimize over both \mathbf{c} and ϕ simultaneously.

3.1 Background on graph cuts and terminology

Graph cuts is a well known optimization problem. Due to a duality theorem by Ford and Fulkerson [29], there are several fast algorithms for this problem. It was introduced as a computer vision tool by Greig et. al. [21] in connection with markov random fields [20]. It has later been studied by Kolmogorov et. al. [2, 27], and has recently received a lot of attention due to its connection with continuous variational problems and PDEs [3, 4, 6, 17, 25]. Its applications range from stereo vision [26], segmentation [1, 24, 51, 16] to noise removal [6, 17]

A graph $\mathcal{G} = (\mathcal{V}, \mathcal{E})$ is a set of vertices \mathcal{V} and a set of edges \mathcal{E} . We let (a, b) denote the edge going from vertex a to vertex b , and let $c(a, b)$ denote the cost (weight) on this edge. In the graph cut scenario there are two distinguished vertices in \mathcal{V} , called the source $\{s\}$ and the sink $\{t\}$. A cut on \mathcal{G} is a partition of the vertices \mathcal{V} into two disjoint sets $(\mathcal{V}_s, \mathcal{V}_t)$ such that $s \in \mathcal{V}_s$ and $t \in \mathcal{V}_t$. For a given cut, the set of severed edges \mathcal{C} is defined as

$$\mathcal{C} = \{(a, b) \mid a \in \mathcal{V}_s, b \in \mathcal{V}_t \text{ and } (a, b) \in \mathcal{E}\}. \quad (18)$$

We say that the cut severs the edge e if e is contained in \mathcal{C} . The cost of the cut is defined as

$$|\mathcal{C}| = \sum_{e \in \mathcal{C}} c(e). \quad (19)$$

We are interested in finding the cut of minimum cost on \mathcal{G} , from now on called the minimum cut. The duality theorem by Ford and Fulkerson [29] states this is equivalent to finding the maximum flow from $\{s\}$ to $\{t\}$, with edge weights indicating bounds on the maximum amount of flow that can be pushed through the edges. Cuts of minimum cost can thus be computed very efficiently by max-flow algorithms such as Ford-Fulkerson [29]. See [2] for a detailed discussion about implementation.

3.2 Discretization of energy functional

We want a discrete representation of the energy functional (11), by restricting the level set function to take values on a uniform grid. Let $\mathcal{P} = \{(i, j) \mid i \in \{1, \dots, N\}, j \in \{1, \dots, M\}\}$ be the set of grid points, and $\delta = 1$ be the mesh size. Correspondingly, $\phi_{i,j}$, $u_{i,j}^0$ and $u_{i,j}$ denote values of functions at the grid points. We would ideally like a discrete version of TV_2

$$TVd_2(\phi) = \sum_{i,j} \delta \sqrt{|\phi_{i+1,j} - \phi_{i,j}|^2 + |\phi_{i,j+1} - \phi_{i,j}|^2}. \quad (20)$$

However, this form is not graph representable. Instead we can consider the anisotropic total variation

$$TVd_1(\phi) = \sum_{i,j} \delta \{|\phi_{i+1,j} - \phi_{i,j}| + |\phi_{i,j+1} - \phi_{i,j}|\}, \quad (21)$$

or the more isotropic version

$$\begin{aligned}
TVd_{1, \frac{\pi}{4}}(\phi) &= \frac{1}{2} \sum_{i,j} \delta \{ |\phi_{i+1,j} - \phi_{i,j}| + |\phi_{i,j+1} - \phi_{i,j}| \} \\
&+ \frac{1}{2\sqrt{2}} \sum_{i,j} \delta \{ |\phi_{i+1,j+1} - \phi_{i,j}| + |\phi_{i+1,j-1} - \phi_{i,j}| \}.
\end{aligned} \tag{22}$$

Using (22), the discrete version of (11) can now be written

$$E_d(\mathbf{c}, \phi) = \sum_{i,j} \delta^2 |u_{i,j} - u_{i,j}^0|^2 + \nu TVd_{1, \frac{\pi}{4}}(\phi). \tag{23}$$

where $u_{i,j}$ is related to $\phi_{i,j}$ and \mathbf{c} by (9).

For a given $p = (i, j) \in \mathcal{P}$, let $\mathcal{N}_k(p)$ for $k = 4$ or 8 be the set of neighboring points of p defined as:

$$N_4(p) = \{(i \pm 1, j), (i, j \pm 1)\}, \text{ and } N_8(p) = \{(i \pm 1, j), (i, j \pm 1), (i \pm 1, j \pm 1)\}.$$

The modification of the definition for boundary points is clear. Using this notation, (23) can be written more compactly

$$E_d(\mathbf{c}, \phi) = \sum_{p \in \mathcal{P}} \delta^2 (u_p - u_p^0)^2 + \nu \sum_{p \in \mathcal{P}} \sum_{q \in \mathcal{N}_k(p)} \frac{1}{2} w_{pq} |\phi_p - \phi_q|, \tag{24}$$

where $w_{pq} = \frac{4\delta^2}{k||p-q||_2}$. Thus the last summation is $TVd_1(\phi)$ for $k = 4$ and $TVd_{1, \frac{\pi}{4}}(\phi)$ for $k = 8$. Since $w_{pq} = w_{qp}$, each term is being counted twice in the last summation. This is compensated by multiplication by the factor $\frac{1}{2}$.

Remark 1. In case of 2-phase segmentation, $TV_{1, \frac{\pi}{4}}$ and TV_1 approximates the perimeter of the interface between the phases. A different approach to approximate the curve length was given in [3], by using a result from integral geometry called the Cauchy-Crofton formula. Their approach do not rely on level set functions. Interestingly, they derive the same coefficients w_{pq} , with the exception of a factor close to one dependent on the angle between the neighboring directions. For both $TVd_{1, \frac{\pi}{4}}$ and TVd_1 , this angle is uniform in all directions.

In the following sections, we show that the minimizer of (23) can be obtained by finding the minimum cut over an appropriate graph, i.e. we will construct a graph \mathcal{G} such that

$$\min_{\mathcal{C} \text{ cut on } \mathcal{G}} |\mathcal{C}| = \min_{\phi} E_d(\mathbf{c}, \phi) + \sigma, \tag{25}$$

where σ is a constant that will be specified later. Note that the minimizer ϕ is not affected by this constant.

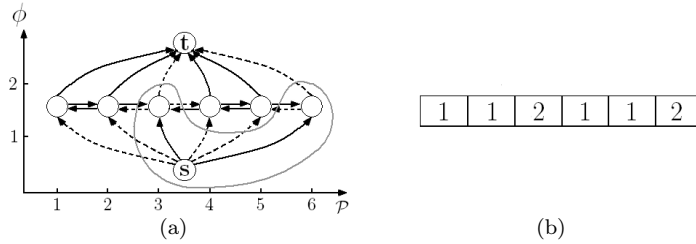


Figure 1: (a) The graph corresponding to a 1D signal of 6 grid points used for two phase segmentation. Edges in \mathcal{E}_D are depicted as vertical arrows and edges in \mathcal{E}_R are depicted as horizontal arrows. The gray curve is used to visualize the cut, vertices in the interior to the curve belongs to \mathcal{V}_s , vertices in the exterior to the curve belongs to \mathcal{V}_t . Edges in \mathcal{C} are depicted as dotted arrows. Figure (b) shows the values of ϕ at each grid point corresponding to the cut in (a), they are determined from definition 3.1

3.3 Graph cuts for 2 phases

We start by showing how graph cut algorithms can be used to minimize (23) in case of $n = 2$. The graph construction is particularly easy in this case. The extension to more than 2 phases will later be regarded as a generalization.

Since any cut naturally separates the graph in two parts, we can associate each grid point p with a vertex v_p . The set of all vertices is thus defined as

$$\mathcal{V} = \{v_p \mid p \in \mathcal{P}\} \cup \{s\} \cup \{t\}.$$

Edges are added from the source to every vertex, and from every vertex to the sink. Edges are also added between vertices corresponding to neighboring grid points.

$$\mathcal{E} = \{(v_p, v_q) \mid p \in \mathcal{P}, q \in \mathcal{N}_k(p)\} \cup \{(s, v_p) \mid \forall p \in \mathcal{P}\} \cup \{(v_p, t) \mid \forall p \in \mathcal{P}\}$$

The relationship between a cut on \mathcal{G} and the level set function ϕ can now be established.

Definition 3.1. Let $(\mathcal{V}_s, \mathcal{V}_t)$ be a cut on \mathcal{G} and \mathcal{C} the set of severed edges. For any grid point $p \in \mathcal{P}$, the corresponding level set function ϕ is defined as

$$\phi_p = \begin{cases} 1 & \text{if } (s, v_p) \in \mathcal{C}, \\ 2 & \text{if } (v_p, t) \in \mathcal{C}. \end{cases} \quad (26)$$

For illustration purposes, the graph corresponding to a 1D signal of six grid points, $\mathcal{P} = \{1, 2, \dots, 6\}$, is displayed in Figure 1(a). In 1D, the neighborhood system reduces to $\mathcal{N}_2(p) = \{p \pm 1\}$. In Figure 1(b) the values of ϕ corresponding to the cut on this graph are shown.

By setting the following edge weights, the equality (25) can be established with $\sigma = 0$

$$\begin{aligned} c(s, v_p) &= \delta^2 |u_p^0 - c_1|^2, & \forall p \in \mathcal{P}, \\ c(v_p, t) &= \delta^2 |u_p^0 - c_2|^2, & \forall p \in \mathcal{P}, \\ c(v_p, v_q) &= \nu w_{pq}, & \forall p \in \mathcal{P}, \quad \forall q \in \mathcal{N}_k(p), \end{aligned} \quad (27)$$

i.e. for any cut and its corresponding ϕ , we have

$$|\mathcal{C}| = E_d(\mathbf{c}, \phi). \quad (28)$$

Therefore, the function ϕ corresponding to a minimum cut on this graph, is a minimizer of the energy function (23).

This type of graph construction for binary optimization problems is well known. There has also been some work on graph cut optimization for the 2-phase Mumford-Shah functional [6, 51].

3.4 Graph cuts for more than 2 phases

The extension to more than two phases ($n > 2$) poses a fundamental problem. Regularizing each characteristic function as in (10) can be seen as a multi-way cut problem, which is shown to be \mathcal{NP} hard [15]. The usual graph cut approach to optimization problems of several labels, is to use some sort of approximation method. The idea is to solve a sequence of binary minimization problems, eventually converging to a suboptimal approximate solution in polynomial time. One of these methods is the so called alpha expansion, which has a linear convergence rate in the number of labels [5]. Some improvements of this method can be found in [28]. A similar method, which has a logarithmic convergence rate in the number of labels can be found in [30]. See [14] for some other integer optimization methods which has been used for image analysis, one of them based on Lagrangian relaxation.

It is difficult to analyze how close the approximate solution is to the exact for these methods, although there are some bounds on the maximum error. Our approach is different in that we construct a numerical method for finding an exact solution. We will instead do the approximation directly in the model, namely by regularizing ϕ as in (11). Previous experiments have shown that this is indeed a very good approximation when the number of phases is not too large. The exact minimum of (23) will be obtained by finding the cut on a special graph. Some similar graph constructions has been given by Ishikawa in [23, 24]. Some of the differences is that our graph consists of less vertices and edges, and is a generalization from the binary case.

Our graph cut approach is based on a strikingly similar idea as the level set method [40]. We will introduce an extra dimension to take care of the difficulties associated with several phases. First note that a piecewise constant level set function ϕ , representing a family of interfaces in \mathbb{R}^d can be regarded as a surface $S_\phi = \{ (x, z) \in \mathbb{R}^d \times \mathbb{R} \mid \phi(x) - z = 0 \}$ embedded in \mathbb{R}^{d+1} . The idea is to represent this surface implicitly on a grid in \mathbb{R}^{d+1} by another

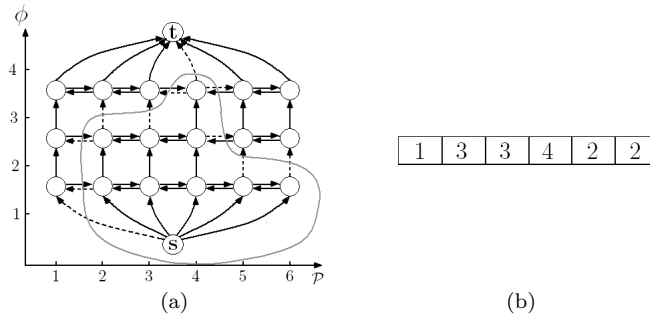


Figure 2: (a) The graph corresponding to a 1D signal of 6 grid points used for 4 phase segmentation. Edges in \mathcal{E}_D are depicted as vertical arrows and edges in \mathcal{E}_R are depicted as horizontal arrows. The gray curve is used to visualize the cut, vertices in the interior to the curve belongs to \mathcal{V}_s , vertices in the exterior to the curve belongs to \mathcal{V}_t . Edges in \mathcal{C} are depicted as dotted arrows. Figure (b) shows the values of ϕ at each grid point corresponding to the cut in (a), they are determined from definition 3.2

higher dimensional level set function. This higher dimensional function will be estimated in a somewhat similar fashion as in Section 3.3. In order to explain the idea in more details, recall that ϕ is defined on the 2D grid $\mathcal{P} = \{(i, j) \mid i \in \{1, \dots, N\}, j \in \{1, \dots, M\}\}$. We want to use ϕ to partition this grid into n phases as in (6). We regard ϕ as a surface in \mathbb{R}^3 , implicitly defined on a 3D grid. For notational convenience, this 3D grid is defined as $\{(p, \ell) \in \mathbb{R}^2 \times \mathbb{R} \mid p \in \mathcal{P}, \ell \in \{1, \dots, n-1\}\}$. As we can see, the grid consists of $MN(n-1)$ grid points. The reason for choosing $n-1$ grid points in the z direction will soon become clear.

As in Section 3.3 we let each vertex correspond to a grid point (p, ℓ) . Such a vertex will be denoted $v_{p,\ell}$. The set of vertices \mathcal{V} is formally defined as

$$\mathcal{V} = \{v_{p,\ell} \mid p \in \mathcal{P}, \ell \in \{1, \dots, n-1\}\} \cup \{s\} \cup \{t\}.$$

An illustration in case of a 1D image where $\mathcal{P} = \{1, 2, \dots, 6\}$, is shown in Figure 2. For ease of visualization, no 2D cases are shown.

The edges are arranged in two groups, \mathcal{E}_D and \mathcal{E}_R . The first group \mathcal{E}_D corresponds to the data term in (24). It is defined as

$$\mathcal{E}_D = \cup_{p \in \mathcal{P}} \mathcal{E}_p,$$

where for each $p \in \mathcal{P}$ the edge set \mathcal{E}_p is defined as

$$\mathcal{E}_p = (s, v_{p,1}) \cup_{\ell=1}^{n-2} (v_{p,\ell}, v_{p,\ell+1}) \cup (v_{p,n-1}, t).$$

The edges in \mathcal{E}_D are illustrated as the vertical arrows in Figure 2. The second group of edges \mathcal{E}_R corresponds to the regularization term in (23). These are

illustrated as the horizontal arrows in Figure 2, i.e.

$$\mathcal{E}_R = \{(v_{p,\ell}, v_{q,\ell}) \mid p \in \mathcal{P}, q \in \mathcal{N}_k(p), \ell \in \{1, \dots, n-1\}\}.$$

For each $p \in \mathcal{P}$, any cut on \mathcal{G} must sever at least one edge from \mathcal{E}_p , otherwise $\{s\}$ and $\{t\}$ are not separated. As a consequence, any cut must sever at least MN edges in \mathcal{E}_D . We say that a cut is admissible if it severs exactly one edge in \mathcal{E}_p for each $p \in \mathcal{P}$, in which case exactly MN edges from \mathcal{E}_D are severed. The cut shown in Figure 3 is not admissible. It severs more than one edge from \mathcal{E}_p for some of the grid points.

Similarly as in Section 3.3, we can now establish the relationship between a cut on \mathcal{G} and a level set function ϕ .

Definition 3.2. Let $(\mathcal{V}_s, \mathcal{V}_t)$ be an admissible cut on \mathcal{G} , and let $\mathcal{C} \subset \mathcal{E}$ be the set of severed edges. For any grid point $p \in \mathcal{P}$, the corresponding level set function ϕ is defined as

$$\phi_p = \begin{cases} 1 & \text{if } (s, v_{p,1}) \in \mathcal{C}, \\ \ell + 1 & \text{if } (v_{p,\ell}, v_{p,\ell+1}) \in \mathcal{C}, \\ n & \text{if } (v_{p,n-1}, t) \in \mathcal{C}. \end{cases} \quad (29)$$

Because of the admissible cut requirement, any such ϕ is single valued. In order to exclude non-admissible cuts, we set the value

$$\sigma = M \cdot N \cdot (n-1) \cdot k \cdot \nu \cdot \max_{p \in \mathcal{P}, q \in \mathcal{N}_k(p)} w_{pq}. \quad (30)$$

We can now define the edge costs (weights) such that the relationship (25) is satisfied. We start by edges in \mathcal{E}_D , i.e. the data edges

$$\begin{aligned} c(s, v_{p,1}) &= \delta^2 |u_p^0 - c_1|^2 + \frac{\sigma}{MN} & \forall p \in \mathcal{P}, \\ c(v_{p,\ell}, v_{p,\ell+1}) &= \delta^2 |u_p^0 - c_\ell|^2 + \frac{\sigma}{MN} & \forall p \in \mathcal{P}, \quad \forall \ell \in \{1, \dots, n-2\}, \\ c(v_{p,n}, t) &= \delta^2 |u_p^0 - c_n|^2 + \frac{\sigma}{MN} & \forall p \in \mathcal{P}. \end{aligned} \quad (31)$$

The costs (weights) for the regularization edges \mathcal{E}_R are defined by

$$c(v_{p,\ell}, v_{q,\ell}) = \nu w_{pq}, \quad \forall p \in \mathcal{P}, \quad \forall q \in \mathcal{N}_k(p), \quad \forall \ell \in \{1, \dots, n-1\}. \quad (32)$$

By the choice of σ , cuts on \mathcal{G} of minimum cost are all admissible. They must sever exactly one edge from \mathcal{E}_p for each $p \in \mathcal{P}$, otherwise a cut of lesser cost exists. This is because the cost of severing one edge in \mathcal{E}_D is higher than the cost of severing $k \cdot (n-1)$ edges in \mathcal{E}_R . Non-admissible cuts, such as the one depicted in Figure 3, cannot be a minimum cut.

To summarize, for any piecewise constant level set function ϕ taking values in $\{1, 2, \dots, n\}$, there exists a unique admissible cut on \mathcal{G} . Moreover, the function ϕ and its corresponding cut satisfies

$$|\mathcal{C}| = E_d(\mathbf{c}, \phi) + \sigma. \quad (33)$$

Thus, we see that a function ϕ corresponding to a minimum cut, is a minimizer of the functional (23), i.e. it solves the segmentation problem. Note that in case $n = 2$, the extra dimension breaks down, and the graph becomes identical to the binary construction.

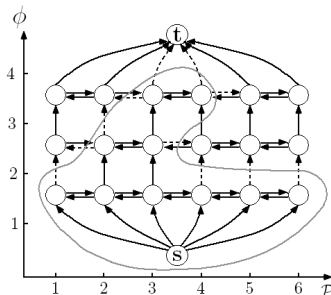


Figure 3: For this 1D example, any cut must sever at least 6 edges in \mathcal{E}_D . Admissible cuts must sever exactly 6 edges in \mathcal{E}_D . The cut shown is not admissible as 7 edges in \mathcal{E}_D are severed

3.5 Algorithm for minimizing the Mumford-Shah functional

The algorithm presented in the last section minimizes $E_d(\mathbf{c}, \phi)$ with respect to ϕ for a fixed \mathbf{c} . Vice versa, for a fixed ϕ the values \mathbf{c} minimizing $E_d(\mathbf{c}, \phi)$ are given by

$$c_i = \frac{\int_{\Omega} u^0(x) \psi_i(x) dx}{\int_{\Omega} \psi_i(x) dx} \quad i = 1, 2, \dots, n, \quad (34)$$

or in discrete form

$$c_i = \frac{\sum_{p \in \mathcal{P}} u_p^0 \psi_{i,p}}{\sum_{p \in \mathcal{P}} \psi_{i,p}} \quad i = 1, 2, \dots, n. \quad (35)$$

We want an algorithm to minimize both with respect to ϕ and \mathbf{c} . This is achieved by combining the two above results in the following iterative descent algorithm.

Algorithm 1. Estimate initial values \mathbf{c}^0 , set $l = 0$.

while($\|\mathbf{c}^l - \mathbf{c}^{l-1}\| < tol$)

1. Use graph cuts to estimate ϕ from

$$\phi = \arg \min_{\tilde{\phi}} E_d(\mathbf{c}^l, \tilde{\phi}). \quad (36)$$

2. Update \mathbf{c}^{l+1} according to equation (35).
3. Update $l \leftarrow l + 1$.

In all our experiment, this algorithm converged in 4-12 iterations. The value of tol can for instance be set to machine precision. It must be noted that this

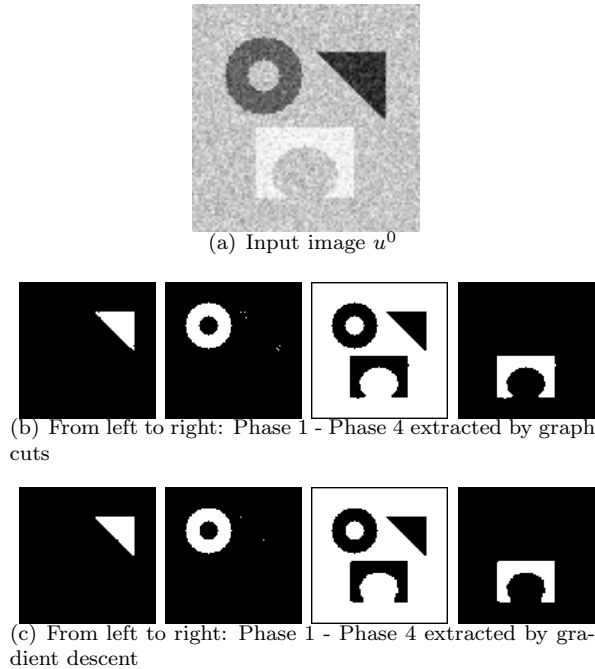


Figure 4: Experiment 1: In (b) and (c), each phase is depicted as a bright region.

algorithm is no longer guaranteed to find the global minima. Theoretically it may get trapped in a local minima close to the initial values \mathbf{c}^0 . However, in practice it is usually rather insensitive to initialization. The initial values \mathbf{c}^0 are computed very efficiently by the isodata algorithm, see [22, 48].

In order to speed up the computation, TV_1 can be used to regularize ϕ in all iterations of Algorithm 1 until $\|\mathbf{c}^l - \mathbf{c}^{l-1}\|$ reaches a small threshold. Only in the final iterations is it necessary to use the more computationally demanding $TV_{1, \frac{\pi}{4}}$ norm.

4 Numerical experiments

In this section we validate our new optimization method by numerical experiments on synthetic and real data. The results are compared with the original gradient descent approach presented in [34, 32]. The implementation of both these methods is made in C++. Comparisons are made both with respect to quality and computation time on an intel 2.19 GHz laptop. The list of computation times is shown in Table 4.

In all graph cut experiments, ϕ is regularized using the combination of the

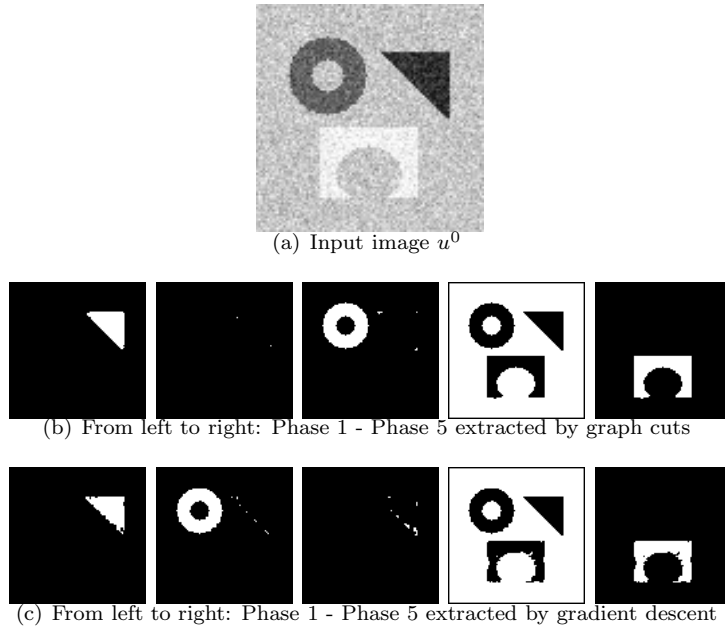


Figure 5: Experiment 2: In (b) and (c) each phase is depicted as a bright region.

TV_1 norm and the $TV_{1,\frac{\pi}{4}}$ norm as explained in Section 3.5. In the gradient descent experiments, the TV_2 norm is used to regularize each ψ_i as in (10). All images are scaled between 0 and 255, and a mesh size of $\delta = 1$ is used.

In the first experiment, we evaluate segmentation results on a synthetic image of 4 regions corrupted by gaussian noise, see Figure 4(a). The segmentation results from graph cut optimization 4(b) is as good as the results from the PDE approach 4(c). As we can see, sharp corners and inside holes are captured with no problem. Traditional level set methods would need to use two level set functions and solve two coupled nonlinear PDEs. For our approach we do not need to solve any PDEs, and one level set function is enough. As can be seen from Table 4, c.f. "Experiment1", the computation time for graph cuts is a lot faster than for PDEs [34].

Next we investigate how the method handles situations where the number of phases is unknown. This can be achieved by minimizing the Mumford-Shah functional with more phases than necessary, hopefully leading to some empty phases. In Figure 5(b)(c) the image from the last experiment has been processed using a 5-phase segmentation approach. With the exception of a few misclassifications, the correct regions gets extracted by phase 1,3,4,5 with second phase becoming empty for graph cuts. Interestingly, gradient descent [34] results in the third phase becoming empty. Computationally, graph cuts are much cheaper, see "Experiment2" in Table 4. An advantage of representing in-

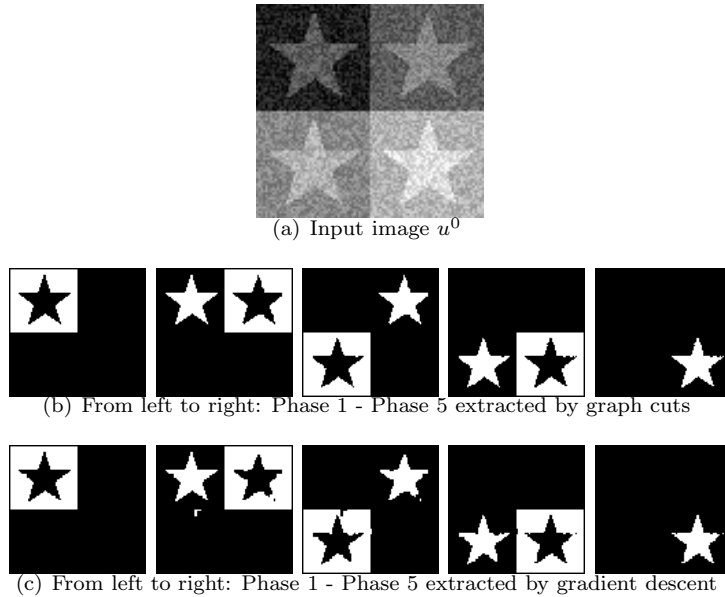
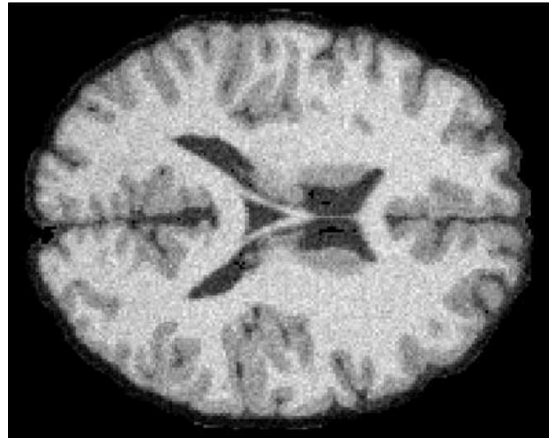


Figure 6: Experiment 3: In (b) and (c), each phase is depicted as a bright region.

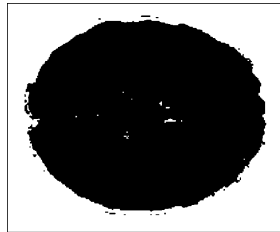
terfaces by the level set method, is its ability to deal with unknown topology. In Figure 6, we seek a partitioning of the image where three of the regions clearly are disconnected. As we can see, both graph cuts and gradient descent are able to extract the correct phases by finding the most suitable topology of the curves. See "Experiment3" in Table 4 for comparison of the execution times.

So far, we have only discussed artificial images where the resolution is quite low. Next we apply our method to a real brain MR image of high resolution. For such a brain image, one would like to extract 3 different tissue classes. This can be achieved by using a 4-phase image segmentation approach. The regions one would like to extract can be classified as: region 1; background, region 2; cerebrospinal fluid, region 3; gray matter and region 4; white matter. As shown in Figure 7, we get almost identical results as the PDE approach [34]. The computation time, on the other hand, is dramatically improved, as can be seen in the row for "Brain" in Table 4.

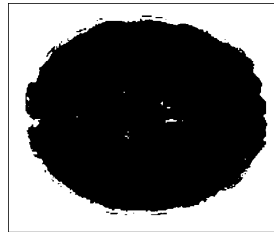
We conclude this section by showing two experiments for the special case of two-phase segmentation, see Figure 8, 9. In the satellite image of Europe in Figure 8, one of the regions is characterized by a scattered set of light point. Our goal is to merge this scattered set into a larger object, constituting the land area of Europe. For this kind of image, edges give very little information about the actual regions. Thus we expect a region based segmentation model like the Mumford-Shah to give the best results. The result of graph cut optimization of



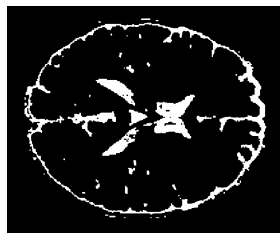
(a) Input noisy MR-image



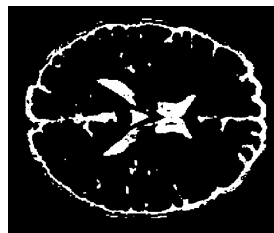
(b) Phase 1 graph cut



(c) Phase 1 PDE



(d) Phase 2 graph cut



(e) Phase 2 PDE



(f) Phase 3 graph cut



(g) Phase 3 PDE



(h) Phase 4 graph cut



(i) Phase 4 PDE

Figure 7: Brain: In (b)-(i), each phase is depicted as a bright region.



Figure 8: (a) Europe by night. (b) Graph cut segmentation with low regularization $\nu = 8 \cdot 10^5$. (c) Graph cut segmentation with high regularization $\nu = 1.5 \cdot 10^6$.

the Mumford-Shah functional is shown in Figure 8 for different regularization parameters. As can be seen, we are able to extract the land continent of Europe in the first region, and the ocean in the second region.

Finally, in Figure 9 we show how the method performs for extracting text from a newspaper. Because of its very high efficiency, this shows the method has potential for becoming competitive in the preprocessing step of reading text from photographic sources.

To summarize, all experiments show that the quality of results for graph cut optimization is as good as PDE based optimization for PCLSM applied to multiphase 2D image segmentation. Furthermore, in the graph cut approach, no parameters need to be tuned and a global minimizer is always found for given values \mathbf{c} .

Comparing the computational cost, graph cuts is several hundreds of times faster than gradient descent. We have not made comparison with any of the fast acceleration schemes such as AOS [31, 11], MBO [45] or Newton [47, 46, 45]. Although the improvement should be less dramatic in these cases, we believe graph cuts is the fastest optimization method to current date. Compared with an optimized matlab implementation of AOS, the graph cut method is at least 40-50 times faster.

	Size	Phases	Gradient descent	Graph Cut
Experiment1	100x100	4	50.3	0.12
Experiment2	100x100	5	70.0	0.179
Experiment3	92x98	5	55.4	0.165
Brain	671x531	4	1988	15.74

Table 1: Computation times in seconds for gradient descent vs graph cut optimization



Figure 9: (a) A page from newspaper, (b) segmentation of the letters using graph cuts.

5 Conclusions

In this work, we have presented a new minimization method for the piecewise constant level set representation of the multiphase Mumford-Shah functional. This minimization method is based on graph cuts. Numerical experiments demonstrated the method is superior in efficiency compared to previous PDE approaches, while maintaining the same quality of results. We have aimed to further unify graph cuts and the level set method. Future work will be generalization of the method to other inverse problems, and other applications of the level set method.

References

- [1] Y. Boykov and G. Funka-Lea. Graph cuts and efficient n-d image segmentation. *Int. J. Comput. Vision*, 70(2):109–131, 2006.
- [2] Y. Boykov and V. Kolmogorov. An experimental comparison of min-cut/max-flow algorithms for energy minimization in vision. In *Energy Minimization Methods in Computer Vision and Pattern Recognition*, pages 359–374, 2001.
- [3] Y. Boykov and V. Kolmogorov. Computing geodesics and minimal surfaces via graph cuts. In *ICCV '03: Proceedings of the Ninth IEEE International Conference on Computer Vision*, page 26, Washington, DC, USA, 2003. IEEE Computer Society.
- [4] Y. Boykov, V. Kolmogorov, D. Cremers, and A. Delong. An integral solution to surface evolution pdes via geo-cuts. *ECCV06*, pages 409–422, 2006.
- [5] Y. Boykova, O. Veksler, and R. Zabih. Fast approximate energy minimization via graph cuts. In *ICCV (1)*, pages 377–384, 1999.

- [6] A. Chambolle. Total variation minimization and a class of binary mrf models. In *Energy Minimization Methods in Computer Vision and Pattern Recognition*, pages 136–152. Springer Berlin / Heidelberg, 2005.
- [7] T. Chan, M. Moelich, and B. Sandberg. Some recent developments in variational segmentation. In *Image processing based on partial differential equations*, pages 175–210. Springer, 2007.
- [8] T. Chan and L.A. Vese. *Active contours without edges*. IEEE Image Proc., 10, pp. 266-277, 2001.
- [9] T.F. Chan and X.-C. Tai. Level set and total variation regularization for elliptic inverse problems with discontinuous coefficients. *J. Comput. Phys.*, 193(1):40 – 66, 2003.
- [10] K. Chen and X.C. Tai. A nonlinear multigrid method for total variation minimization from image restoration. *J. Sci. Comput.*, 33(2):115–138, 2007.
- [11] O. Christiansen and X.-C. Tai. Fast implementation of piecewise constant level set methods. In *Image processing based on partial differential equations*, pages 253–272. Springer Verlag, 2006.
- [12] D. Cremers, T. Kohlberger, and C. Schnorr. Shape statistics in kernel space for variational image segmentation. *Patt. Recogn.*, 36(10):1929–1943, 2003.
- [13] D. Cremers, N. Sochen, and C. Schnorr. Multiphase dynamic labeling for variational recognition-driven image segmentation. volume 3024, pages 74–86. Springer, 2004.
- [14] G. Dahl, G. Storvik, and A. Fadnes. Large-scale integer programs in image analysis. *Oper. Res.*, 50(3):490–500, 2002.
- [15] E. Dahlhaus, D. S. Johnson, C. H. Papadimitriou, P. D. Seymour, and M. Yannakakis. The complexity of multiway cuts (extended abstract). In *STOC '92: Proceedings of the twenty-fourth annual ACM symposium on Theory of computing*, pages 241–251, New York, NY, USA, 1992. ACM.
- [16] J. Darbon. A note on the discrete binary mumford-shah model. *Proceedings of Computer Vision/Computer Graphics Collaboration Techniques, (MIRAGE 2007), LNCS Series vol. 44182*, pages 283–294, March 2007.
- [17] J. Darbon and M. Sigelle. Image restoration with discrete constrained total variation part i: Fast and exact optimization. *J. Math. Imaging Vis.*, 26(3):261–276, 2006.
- [18] A. Dervieux and F. Thomasset. A finite element method for the simulation of a Rayleigh-Taylor instability. In *Approximation methods for Navier-Stokes problems (Proc. Sympos., Univ. Paderborn, Paderborn, 1979)*, volume 771 of *Lecture Notes in Math.*, pages 145–158. Springer, Berlin, 1980.

- [19] R.P. Fedkiw, G. Sapiro, and C.H. Shu. Shock capturing, level sets, and PDE based methods in computer vision and image processing: a review of Osher's contributions. *J. Comput. Phys.*, 185(2):309–341, 2003.
- [20] S. Geman and D. Geman. Stochastic relaxation, gibbs distributions, and the bayesian restoration of images. In *Readings in uncertain reasoning*, pages 452–472. Morgan Kaufmann Publishers Inc., San Francisco, CA, USA, 1990.
- [21] D. M. Greig, B. T. Porteous, and A. H. Seheult. Exact maximum a posteriori estimation for binary images. *Journal of the Royal Statistical Society, Series B*, pages 271–279, 1989.
- [22] E. Hodneland. *Segmentation of digital images*. Cand. Scient Thesis, Department of Mathematics, University of Bergen. Available online at www.mi.uib.no/tai, 2003.
- [23] H. Ishikawa. Exact optimization for markov random fields with convex priors. *IEEE Transactions on Pattern Analysis and Machine Intelligence*, 25(10):1333–1336, 2003.
- [24] H. Ishikawa and D. Geiger. Segmentation by grouping junctions. In *CVPR '98: Proceedings of the IEEE Computer Society Conference on Computer Vision and Pattern Recognition*, page 125, Washington, DC, USA, 1998. IEEE Computer Society.
- [25] D. Kirsanov and S. Gortler. A discrete global minimization algorithm for continuous variational problems, 2004.
- [26] V. Kolmogorov and R. Zabih. Multi-camera scene reconstruction via graph cuts. In *ECCV '02: Proceedings of the 7th European Conference on Computer Vision-Part III*, pages 82–96, London, UK, 2002. Springer-Verlag.
- [27] V. Kolmogorov and R. Zabih. What energy functions can be minimized via graph cuts? *IEEE Transactions on Pattern Analysis and Machine Intelligence*, 26(2):147–159, 2004.
- [28] N. Komodakis, G. Tziritas, and N. Paragios. Fast, approximately optimal solutions for single and dynamic mrf. *Computer Vision and Pattern Recognition, 2007. CVPR '07. IEEE Conference on*, pages 1–8, 17-22 June 2007.
- [29] D. Fulkerson L. Ford. *Flows in networks*. Princeton University Press, 1962.
- [30] V. Lempitsky, C. Rother, and A. Blake. Logcut - efficient graph cut optimization for markov random fields. *Computer Vision, 2007. ICCV 2007. IEEE 11th International Conference on*, pages 1–8, 14-21 Oct. 2007.
- [31] H. Li and X.C. Tai. Piecewise constant level set method for multiphase motion. *Int. J. Numer. Anal. Model.*, 4(2):291–305, 2007.

- [32] J. Lie, M. Lysaker, and X.C. Tai. Piecewise constant level set methods and image segmentation. In *Scale Space and PDE Methods in Computer Vision*, pages 573–584. Springer, 2005.
- [33] J. Lie, M. Lysaker, and X.C. Tai. A binary level set model and some applications to mumford-shah image segmentation. *IEEE Transactions on Image Processing*, 15(5):1171–1181, 2006.
- [34] J. Lie, M. Lysaker, and X.C. Tai. A variant of the level set method and applications to image segmentation. *Math. Comp.*, 75(255):1155–1174 (electronic), 2006.
- [35] A. Losnegård, O. Christiansen, and X.-C. Tai. Piecewise constant level set method for 3d image segmentation. In *Scale space and variational methods in Computer vision*, F. Sgallari, A. Murli and N. Paragios eds, Springer, pages 687–696, 2007.
- [36] T. Lu, P. Neittaanmaki, and X.-C. Tai. *A parallel splitting up method and its application to navier-stoke equations*. Applied Mathematics Letters, 4:25-29, 1991.
- [37] T. Lu, P. Neittaanmaki, and X.-C. Tai. *A parallel splitting up method for partial differential equations and its application to navier-stokes equations*. RAIRO Math. Model. and Numer. Anal., 26:673-708, 1992.
- [38] D. Mumford and J. Shah. Optimal approximation by piecewise smooth functions and associated variational problems. *Comm. Pure Appl. Math*, 42, 42:577–685, 1989.
- [39] S. Osher and R. Fedkiw. *An overview and some recent results*. J.Comput.Phys, 169 No. 2:463-502, 2001.
- [40] S. Osher and J.A. Sethian. Fronts propagating with curvature dependent speed: algorithms based on hamilton-jacobi formulations. *J. Comput. Phys.*, 79(1):12–49, 1988.
- [41] F. Ranchin, A. Chambolle, and F. Dibos. Total variation minimization and graph cuts for moving objects segmentation. In *Scale Space and Variational Methods in Computer Vision*, pages 743–753. Springer, 2006.
- [42] J.A. Sethian. *Level set methods and fast marching methods*, volume 3 of *Cambridge Monographs on Applied and Computational Mathematics*. Cambridge University Press, Cambridge, second edition, 1999. Evolving interfaces in computational geometry, fluid mechanics, computer vision, and materials science.
- [43] Y. Shi and W.C. Karl. A real-time algorithm for the approximation of level-set-based curve evolution. *IEEE transactions on image processing*, 17(5):645–656, 2008.

- [44] X.-C. Tai and T. F. Chan. A survey on multiple level set methods with applications for identifying piecewise constant functions. *Int. J. Numer. Anal. Model*, 1(1):25–47, 2004.
- [45] X.C. Tai, O. Christiansen, P. Lin, and I. Skjaelaaen. Image segmentation using some piecewise constant level set methods with mbo type of project. *International Journal of Computer Vision*, 73:61–76, 2007.
- [46] X.C. Tai and C. Yao. Image segmentation by piecewise constant Mumford-Shah model without estimating the constants. *J. Comput. Math.*, 24(3):435–443, 2006.
- [47] X.C. Tai and C. Yao. Fast PCLSM with newton updating algorithm. In *Image processing based on partial differential equations*, pages 249–264. Springer, 2007.
- [48] F. R. Dias Velasco. Thresholding using the ISODATA clustering algorithm. *IEEE Trans. Systems Man Cybernet.*, 10(11):771–774, 1980.
- [49] L. A. Vese and T. F. Chan. A new multiphase level set framework for image segmentation via the mumford and shah model. *International Journal of Computer Vision*, 50:271–293, 2002.
- [50] J. Weickert, B. H. Romeny, and M. A. Viergever. Efficient and reliable schemes for nonlinear diffusion filtering. *IEEE Trans. Image Process.*, 7:398–409, 1998.
- [51] N. El. Zehiry, S. Xu, P. Sahoo, and A. Elmaghraby. Graph cut optimization for the mumford-shah model. In *Proceedings of the Seventh IASTED International Conference visualization, imaging and image processing*. Springer Verlag, 2007.